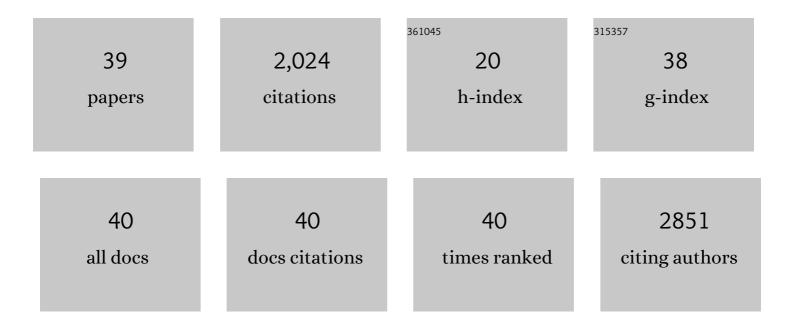
Bin Wei

List of Publications by Year in descending order

Source: https://exaly.com/author-pdf/36615/publications.pdf Version: 2024-02-01



4	#	Article	IF	CITATIONS
	1	Growth of 2D MoP single crystals on liquid metals by chemical vapor deposition. Science China Materials, 2021, 64, 1182-1188.	3.5	15
2	2	Atomic-Step Enriched Ruthenium–Iridium Nanocrystals Anchored Homogeneously on MOF-Derived Support for Efficient and Stable Oxygen Evolution in Acidic and Neutral Media. ACS Catalysis, 2021, 11, 3402-3413.	5.5	87
4	3	Isolated Single-Atom Ni–N ₅ Catalytic Site in Hollow Porous Carbon Capsules for Efficient Lithium–Sulfur Batteries. Nano Letters, 2021, 21, 9691-9698.	4.5	167
2	4	Realizing Few‣ayer Iodinene for Highâ€Rate Sodium″on Batteries. Advanced Materials, 2020, 32, e2004835.	11.1	41
ł	5	Ultrafine oxygen-defective iridium oxide nanoclusters for efficient and durable water oxidation at high current densities in acidic media. Journal of Materials Chemistry A, 2020, 8, 24743-24751.	5.2	45
(6	Universal growth of ultra-thin III–V semiconductor single crystals. Nature Communications, 2020, 11, 3979.	5.8	34
7	7	Bifunctional Porous Cobalt Phosphide Foam for High-Current-Density Alkaline Water Electrolysis with 4000-h Long Stability. ACS Sustainable Chemistry and Engineering, 2020, 8, 10193-10200.	3.2	57
ł	8	Hierarchically structured diamond composite with exceptional toughness. Nature, 2020, 582, 370-374.	13.7	141
Ģ	9	Tunable Mechanical Property and Structural Transition of Silicon Nitride Nanowires Induced by Focused Ion Beam Irradiation. ACS Applied Materials & Interfaces, 2020, 12, 32175-32181.	4.0	1
1	10	Strong Electronic Coupling between Ultrafine Iridium–Ruthenium Nanoclusters and Conductive, Acid-Stable Tellurium Nanoparticle Support for Efficient and Durable Oxygen Evolution in Acidic and Neutral Media. ACS Catalysis, 2020, 10, 3571-3579.	5.5	122
-	11	Mille-Crêpe-like Metal Phosphide Nanocrystals/Carbon Nanotube Film Composites as High-Capacitance Negative Electrodes in Asymmetric Supercapacitors. ACS Applied Energy Materials, 2020, 3, 4580-4588.	2.5	19
-	12	Grain Boundary Induced Ultralow Threshold Random Laser in a Single GaTe Flake. ACS Applied Materials & Interfaces, 2020, 12, 23323-23329.	4.0	10
	13	Inverted Pyramid Textured p-Silicon Covered with Co ₂ P as an Efficient and Stable Solar Hydrogen Evolution Photocathode. ACS Energy Letters, 2019, 4, 1755-1762.	8.8	35
1	14	High-Performance Flexible Solid-State Asymmetric Supercapacitors Based on Bimetallic Transition Metal Phosphide Nanocrystals. ACS Nano, 2019, 13, 10612-10621.	7.3	214
	15	Magnetism and Optical Anisotropy in van der Waals Antiferromagnetic Insulator CrOCl. ACS Nano, 2019, 13, 11353-11362.	7.3	97
-	16	A ternary SnS1.26Se0.76 alloy for flexible broadband photodetectors. RSC Advances, 2019, 9, 14352-14359.	1.7	7
-	17	Large-Scale Fabrication of Hollow Pt ₃ Al Nanoboxes and Their Electrocatalytic Performance for Hydrogen Evolution Reaction. ACS Sustainable Chemistry and Engineering, 2019, 7, 9842-9847.	3.2	14
	18	Phase Identification and Strong Second Harmonic Generation in Pure ε-InSe and Its Alloys. Nano Letters, 2019, 19, 2634-2640.	4.5	86

Bin Wei

#	Article	IF	CITATIONS
19	Synthesis of low-symmetry 2D Ge _(1â^'x) Sn _x Se ₂ alloy flakes with anisotropic optical response and birefringence. Nanoscale, 2019, 11, 23116-23125.	2.8	9
20	Structural Distortion-Induced Charge Gradient Distribution of Co Ions in Delithiated LiCoO ₂ Cathode. Journal of Physical Chemistry Letters, 2019, 10, 7537-7546.	2.1	39
21	Highly Sensitive Polarization Photodetection Using a Pseudo-One-Dimensional Nb _(1–<i>x</i>) Ti _{<i>x</i>} S ₃ Alloy. ACS Applied Materials & Interfaces, 2019, 11, 3342-3350.	4.0	35
22	Disassembly of 2D Vertical Heterostructures. Advanced Materials, 2019, 31, e1805976.	11.1	12
23	Few‣ayer Bismuthene with Anisotropic Expansion for Highâ€Areal apacity Sodiumâ€Ion Batteries. Advanced Materials, 2019, 31, e1807874.	11.1	165
24	Ethylenediamine-Enabled Sustainable Synthesis of Mesoporous Nanostructured Li2FellSiO4 Particles from Fe(III) Aqueous Solution for Li-Ion Battery Application. ACS Sustainable Chemistry and Engineering, 2018, 6, 7458-7467.	3.2	14
25	Growth of 2D GaN Single Crystals on Liquid Metals. Journal of the American Chemical Society, 2018, 140, 16392-16395.	6.6	183
26	In-Plane Optical Anisotropy and Linear Dichroism in Low-Symmetry Layered TlSe. ACS Nano, 2018, 12, 8798-8807.	7.3	64
27	In Situ TEM Investigation of Electron Irradiation Induced Metastable States in Lithium-Ion Battery Cathodes: Li ₂ FeSiO ₄ versus LiFePO ₄ . ACS Applied Energy Materials, 2018, 1, 3180-3189.	2.5	20
28	Strain Gradient Modulated Exciton Evolution and Emission in ZnO Fibers. Scientific Reports, 2017, 7, 40658.	1.6	6
29	Luminescence Properties of GaAs Quantum Dot-in-Nanowire Structure for Quantum Photonics. , 2015, , .		0
30	Enhanced contrast separation in scanning electron microscopes via a suspended-thin sample approach. Ultramicroscopy, 2014, 146, 83-90.	0.8	1
31	Variation of exciton emissions of ZnO whiskers reversibly tuned by axial tensile strain. Optics Express, 2014, 22, 4000.	1.7	8
32	Selfâ€Assembled Quantum Dot Structures in a Hexagonal Nanowire for Quantum Photonics. Advanced Materials, 2014, 26, 2710-2717.	11.1	31
33	Bandgap engineering and manipulating electronic and optical properties of ZnO nanowires by uniaxial strain. Nanoscale, 2014, 6, 4936-4941.	2.8	55
34	Self-assembly of single "square―quantum rings in gold-free GaAs nanowires. Nanoscale, 2014, 6, 3190.	2.8	6
35	Local thermal conductivity of polycrystalline AlN ceramics measured by scanning thermal microscopy and complementary scanning electron microscopy techniques. Chinese Physics B, 2012, 21, 016501.	0.7	1
36	Size-Dependent Bandgap Modulation of ZnO Nanowires by Tensile Strain. Nano Letters, 2012, 12, 4595-4599.	4.5	173

Bin Wei

#	Article	IF	CITATIONS
37	Distinguishing crystallographic misorientations of lanthanum zirconate epilayers on nickel substrates by electron backscatter diffraction. Ultramicroscopy, 2011, 111, 314-319.	0.8	2
38	Charge compensation by in-situ heating for insulating ceramics in scanning electron microscope. Ultramicroscopy, 2009, 109, 1326-1332.	0.8	6
39	Charge Contrast Imaging of Nonconductive Samples in the Highâ€Vacuum Field Emission Scanning Electron Microscope. Scanning, 2007, 29, 230-237.	0.7	2